instruments

CITESCORE
2.6

Article

Design, Construction and Characterization of Sealed Tube Medium Power CO_2 Laser System

Muddasir Naeem, Tayyab Imran, Mukhtar Hussain and Arshad Saleem Bhatti

Special Issue
Photonic Devices Instrumentation and Applications II

Edited by
Dr. Christos Riziotis

MDPI

https://doi.org/10.3390/instruments6040072

instruments

MDPI

Article

Design, Construction and Characterization of Sealed Tube Medium Power CO_2 Laser System

Muddasir Naeem [1,*], Tayyab Imran [1], Mukhtar Hussain [2] and Arshad Saleem Bhatti [3]

[1] Group of Laser Development (GoLD), Department of Physics, Syed Babar Ali School of Science and Engineering, Lahore University of Management Sciences (LUMS), Lahore 54792, Pakistan
[2] Extreme Light Laboratory, Department of Physics and Astronomy, University of Nebraska-Lincoln, Lincoln, NE 68588, USA
[3] M.A. Jinnah Campus, Virtual University, Defence Road, Off Raiwind Road, Lahore 54660, Pakistan
* Correspondence: muddasirnaeem98@gmail.com

Abstract: A low-cost medium-power carbon dioxide (CO_2) laser system is designed, constructed, and characterized to produce coherent, monochromatic laser radiation in the infrared region. The laser cavity is simulated and designed by using ZEMAX optic studio. A switch-mode high-tension pump source is designed and constructed using a flyback transformer and simulated using NI Multisim to study the voltage behavior at different node points. A prototype cooling system/chiller is designed and built using thermo-electric coolers (TEC) to remove the excess heat produced during laser action. Various parameters, such as pumping mechanism, chiller stability, efficiency, output power, and current at different applied voltages, are studied. The chiller efficiency at different output powers of the laser is analyzed, which clearly shows that the chiller's cooling rate is good enough to compensate for the heat generated by the laser system. The center wavelength of the carbon dioxide laser is 10.6 μm with an FWHM of 1.2 nm simulated in the ZEMAX optic studio. The output beam penetration through salt rock (NaCl), wood, and acrylic sheet (PMMA) at various output powers is analyzed to measure the penetration depth rate of the CO_2 laser.

Keywords: optical design; thermoelectric coolers; irradiance; high tension pump source; penetration depth; pulse width modulation

check for updates

Citation: Naeem, M.; Imran, T.; Hussain, M.; Bhatti, A.S. Design, Construction and Characterization of Sealed Tube Medium Power CO_2 Laser System. *Instruments* **2022**, *6*, 72. https://doi.org/10.3390/instruments6040072

Academic Editor: Christos Riziotis

Received: 16 September 2022
Accepted: 28 October 2022
Published: 2 November 2022

Publisher's Note: MDPI stays neutral with regard to jurisdictional claims in published maps and institutional affiliations.

Copyright: © 2022 by the authors. Licensee MDPI, Basel, Switzerland. This article is an open access article distributed under the terms and conditions of the Creative Commons Attribution (CC BY) license (https://creativecommons.org/licenses/by/4.0/).

1. Introduction

The CO_2 laser is one of the most stunning, efficient, and practical lasers discovered to date. The carbon dioxide laser operates in the infrared band and creates a significant quantity of heat, which is employed as a primary property in a variety of applications [1]. Super-pulsed carbon dioxide lasers have been widely employed in medical and aesthetic applications in recent years. Furthermore, carbon dioxide lasers are employed in industrial operations. A system's higher efficiency and operational stability are essential for industrial applications. The most typical use is material cutting. Carbon dioxide laser cutting provides the advantages of excellent accuracy, low incision width, and a smooth surface. As carbon dioxide laser technology matures, it is being utilized in a variety of industries such as industry, health, and agriculture to enhance human spiritual and material civilizations, as well as to improve people's everyday lives and raise mankind to a new level [2,3]. Kumar Patel [4] reported the first CW output of about 1 mW using molecular vibrational-rotational transitions of carbon dioxide (CO_2) electronic ground state [5]. In 1969, Philip L. Hanst and John A. Morreal designed and tested a CO_2 laser system with two gas absorption cells built into the cavity. High-powered pulsed operation at varying wavelengths ranging from 9.08 microns to 10.6 microns at repeat frequencies of up to 100 kHz has been accomplished by the correct range of absorbing gases [6]. A low-pressure continuous-wave CO_2 laser for single-line application was planned and built in 1981. This laser works in a single axial mode with a frequency stabilization of greater than 100 kHz at the peak of the power

profile. The peak power varies from 0.1 to 5 Watts [7]. In 1997, a high-power 24-channel radial array slab RF excited carbon dioxide laser referred to as the Zodiac geometry was built [8]. A transverse flow transversely excited (TFTE) CW CO_2 with a maximum output power of about 15 kW has been developed by A.K. Nath and T. Reghu. The laser was operated up to 15 kW output power in four modes: continuous wave mode, periodic pulse mode, single-shot mode, and processing velocity-dependent power mode with 1.2 kHz modulation bandwidth [9]. A single CO_2 laser beam may generate a record peak power of 15 TW. Using a master oscillator-power amplifier laser system up to 100 J of energy may be extracted in a train of 3 ps laser pulses separated by 18 ps [10]. A low-cost homemade prototype nitrogen laser [11] is designed and fabricated using the air as an active medium to generate a nano-second pulse laser, but the efficiency was low, with a similar approach reported in this article. With the passage of time, the efficiency of CO_2 lasers increased, but commercially available lasers are quite expensive. Unfortunately, the cost of commercially available carbon dioxide lasers is prohibitive for many small industries and educational institutes. Our approach is straightforward in making the CO_2 laser. We used a sealed tube and developed the high-tension pump source and non-conventional cooling system for the tube to fabricate a cost-effective and efficient medium-power CO_2 laser system.

This paper mainly introduces the designing, constructing, and characterizing of a low-cost medium-power CO_2 laser system with a switch-mode power supply and prototype cost-effective homemade chiller. A cost-effective prototype chiller is designed and fabricated using Thermoelectric coolers and small aluminum blocks. Furthermore, this research focuses on the carbon dioxide laser, covering its features, structure, and applications.

2. Design Simulation

2.1. Carbon Dioxide (CO_2) Laser Cavity

The laser cavity design is carried out using Zemax Optic Studio [12] software. When all the surfaces are defined for all relevant parameters involved in the design, the ZEMAX provides a 2D layout [13,14] and a shaded design model [15]. A reflecting mirror, focusing lens, and detector are used to detect and analyze the beam in the design. The incident flux on the surface is referred to as irradiance and is measured as power per unit area. When the applied voltage across the laser cavity increases, more photons are delivered inside the cavity and output power increases linearly.

Figure 1a shows the output power variation with the number of cycles within the cavity designed in the ZEMAX. It shows that with the increase in cycles that cause the stimulated emission in the laser cavity, the output power of the laser beam increases.

The output of the CO_2 laser system lies in the IR region. Figure 1b shows the output beam spectrum of the laser cavity designed in the ZEMAX optic studio. For spectrum, a diffraction grating is placed at the output of the laser cavity. The output beam is resolved into its components, and a Gaussian shape spectrum at the output is obtained.

The simulated result shows the central wavelength at 10.6 μm with an FWHM of 1.2 nm, as shown in Figure 1b, which confirms the emission of the laser system in the IR region. This irradiance plot represents the top view of the Gaussian spectrum, and irradiance changes symmetrically on both sides from the center of the beam spot.

2.2. High-Tension Pump Source

The high-tension pump source circuit is designed and simulated to understand the voltage behavior and its waveform. This circuit Figure 2a is implemented in designing and fabricating the high-tension pump source. NI Multisim electrical/electronic circuit simulation software tools were used for these simulations [16–18].

The graph Figure 2b shows a square wave generation simulation at the output of 555-timer-based pulse width modulation (PWM). The frequency of the square wave voltage can be changed by varying the capacitor or resistance values [11,19,20].

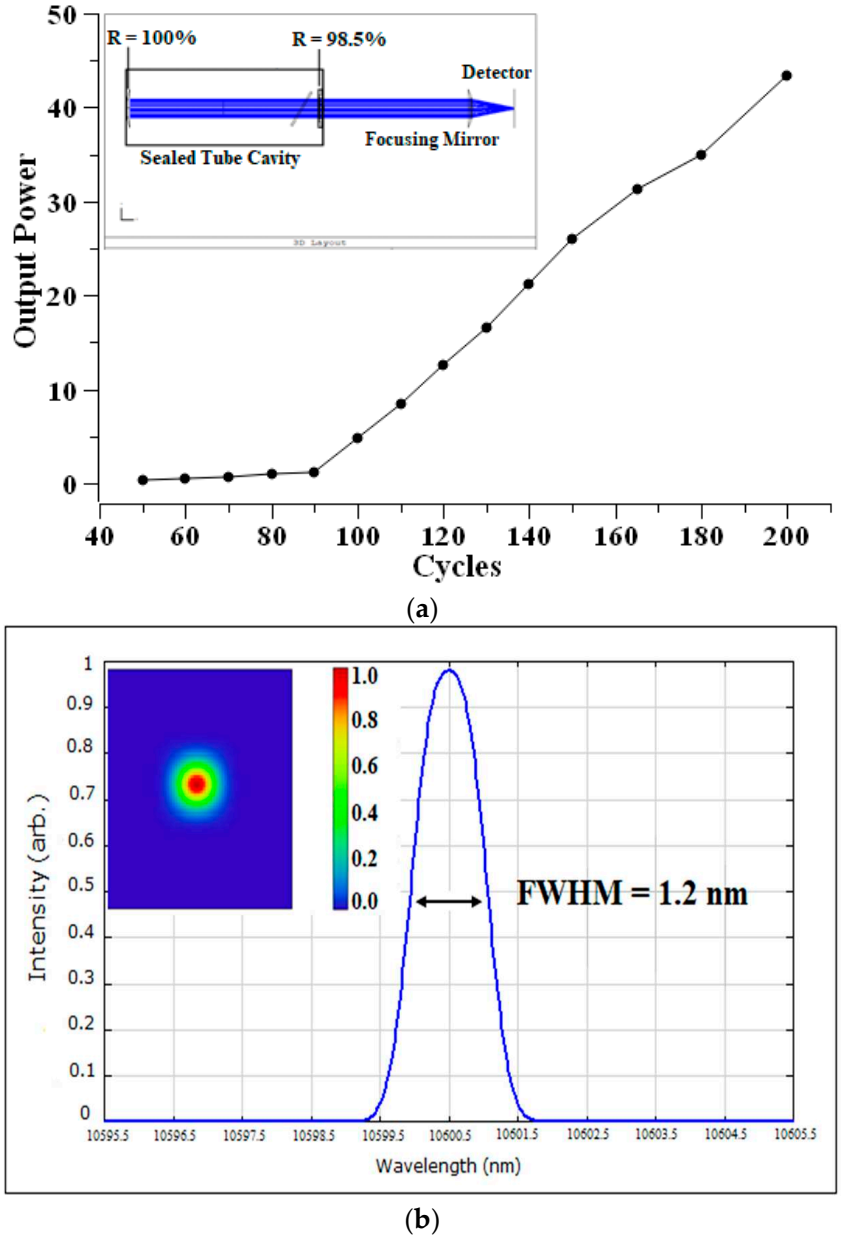

Figure 1. (**a**) Output power variation w.r.t number of cycles in the cavity (inset: 2D layout of the cavity). (**b**) Output beam spectrum of design laser cavity in Zemax Optic Studio (inset: beam spot).

The waveform of the output pulses Figure 2c shows the behavior of the MOSFET IRFZ44 when a PMW's square wave signal is applied to the gate. The gate's voltage Figure 2a controls the drain to the source current [21]. The graph Figure 2d shows the output of 555-timer-based PWM (Blue) and flyback transformer (Red). When the peak of the square wave signal from the PWM approaches the gate of the MOSFET, the current starts flowing in the flyback transformer's primary coil through the drain to the source; during this time, there is no voltage at the output of the flyback transformer. When the square wave signal's lowest point reaches the MOSFET's gate, no current flows through the primary of the flyback transformer. The magnetic field collapses in the core, very high voltage is induced in the secondary coil of the flyback transformer, and the current starts flowing through the load. This cycle is repeated repeatedly to produce high-voltage pulses [22,23].

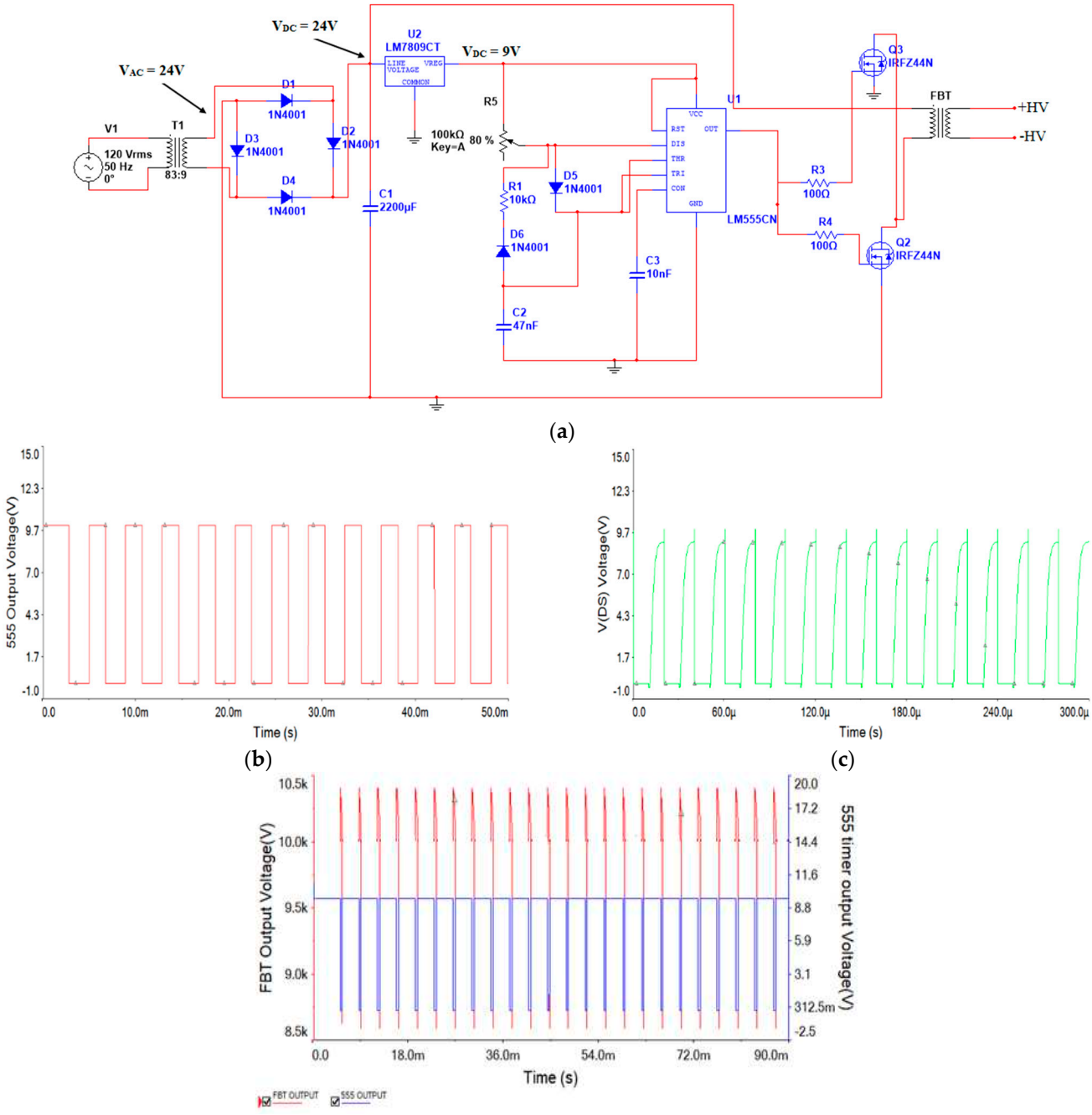

Figure 2. (**a**) Circuit diagram of high-tension pump source; (**b**) pulse width modulation (PWM) output voltage waveform; (**c**) voltage behavior across the drain to source when square wave voltage is applied at the gate of MOSFET; (**d**) output voltage waveform of PWM and flyback transformer.

3. Prototype Cooling System for Laser Tube

A large amount of heat is produced during the laser operation, affecting the laser's stability. A prototype cooling system is designed to remove this excess heat. The heat produced at different rates in the laser tube's cavity depends on the output power of the laser system. As the output power increases, the heat generated in the laser tube's cavity also increases. An efficient cooling system is designed and constructed using thermoelectric coolers. The chiller's cooling rate is 0.7 °C/min, which is enough to compensate for the heat generated in the cavity and make it stable for an extended period of its operation. The cooling system is shown in Figure 3a.

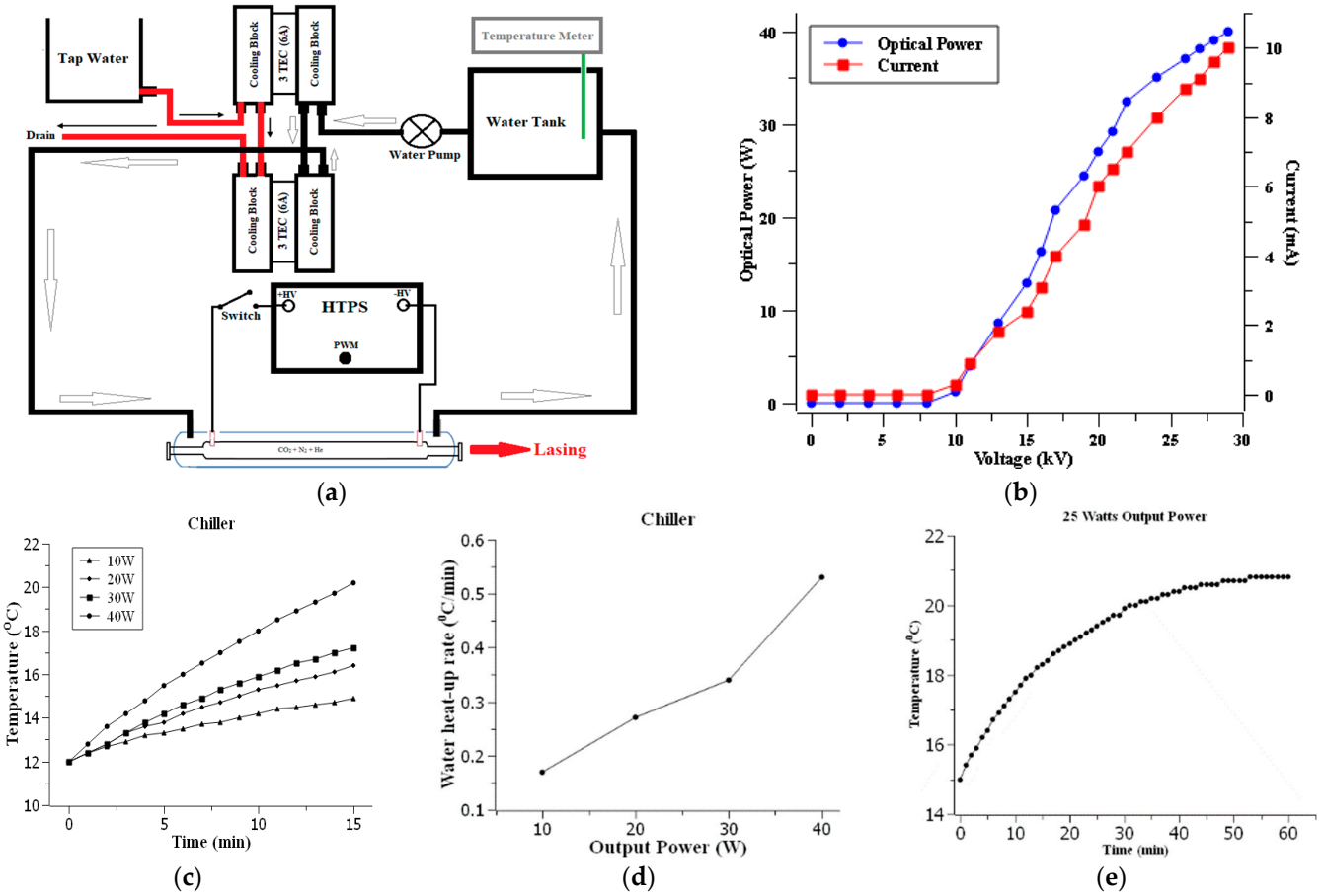

Figure 3. (**a**) Complete laser system with cooling system and high-tension pump source connections. (**b**) Variation of laser output power and current along applied voltage. (**c**) Variation in water temperature circulating in the tube along output power of the laser. (**d**) Output power vs. water heat-up rate. (**e**) Chiller behavior at a moderate output power for an extended period of operation.

Six thermoelectric coolers and four aluminum blocks are used to design the cooling system. A set of three thermoelectric coolers (TEC) are sandwiched between the two aluminum blocks. In the cooling system, the water circulates in two loops. The de-ionized water is stored in the water tank. A water pump is attached to the water tank. The water is pumped from the tank and circulates in the aluminum block connected to the cold side of the thermoelectric coolers. The heat is extracted from the water when it circulates in the aluminum blocks. The extracted heat is transferred to the hot side of the thermoelectric coolers. The de-ionized water is made to pass through another aluminum block connected to the cold side of the thermoelectric coolers. The cold water through pipes circulates in the laser tube, extracts heat from the laser cavity, and goes back to the water tank. Another aluminum block is attached to remove the heat from the hot side of the thermoelectric coolers. Tap water circulates in the aluminum block attached to the hot side of the thermoelectric coolers, extracts the heat from the hot side, and enhances efficiency. This cycle repeats continuously, and the cooling system efficiently removes the heat produced in the laser cavity during laser action.

The graph Figure 3c compares the water temperature circulating in the tube at different output powers. Initially, the water temperature was 12 °C. As the laser output power increases, more heat is produced, and the water temperature rises slowly. The cavity is stable because the water temperature is maintained at a certain level at which it can compensate for the heat produced by the laser action. The graph Figure 3d shows that the water heating rate increases with the laser's output power. The laser can be operated for an extended period without any problem. In the graph Figure 3e, the cooling efficiency

during the extended period of laser operation is shown. The chart shows that the water temperature increased with time and became stable at one point, after which the cooling rate of the chiller became equal to the heating rate of water. The output power of the laser system remains stable during that period.

4. Results

4.1. Characterization of the Laser System

The block diagram Figure 3a shows the chiller, laser tube, and high-tension pump source connections. A sealed laser tube is used, which is filled with carbon dioxide (CO_2), nitrogen (N_2), and helium (He). The CO_2, N_2, and He ratios are 1:2:7, respectively. The high-tension pump source is connected to the electrodes of the laser tube. The cooling system is associated with the tube through pipes, black to extract the heat from the cavity and red to extract the heat from the hot side of the thermoelectric cooler to improve efficiency. Specification of the sealed laser tube is given in Table 1.

Table 1. Specifications of sealed laser tube.

Power	**40 W**
Length	70 cm
Outer Cylinder Diameter	5 cm
Inner Cylinder Diameter	2 cm
Triggering Voltage	9 kV
Working Voltage	10 kV
Power Stability	±5%
Triggering Current	5 mA
Maximum Working Current	20 mA
Spot Diameter	4 mm

Figure 3b plots the current, output power, and applied voltage behavior. When the applied voltage is less than the threshold voltage, a small amount of current flows through the laser tube, and the output power is zero. At the threshold applied voltage, the current reaches the value required to produce electric discharge through the gas, and the lasing action starts in the cavity. Beyond the threshold voltage, the laser system's current and output power increases with applied voltage. The graph shows that the threshold voltage of the laser system is 9 kV, and output power increases with the applied voltage. The maximum output power of the laser system is 40 watts at a current of 10 mA, as shown in Figure 3b [24]. The output power increases linearly with the applied voltage. The increased applied voltage increases the discharge through the gas, resulting in the excited state of CO_2 molecules getting heavily populated. In this process, a large number of photons are generated in the cavity and the power of the output beam increases [25,26].

4.2. Penetration Rate of Output Beam through Different Materials

The carbon dioxide laser is frequently used for cutting because of its high power [27]. The laser beam's penetration depth at different output powers through the pink salt (NaCl) rock, acrylic sheet (PMMA), and wood are analyzed.

The most important factors that affect the beam penetration through the material are laser power, cutting speed, focal position, focal length, and the distance between the laser and the cut material. Besides that, material properties such as thickness, tensile strength, melting point, and optical properties also affect the penetration rate through different materials. The graphs Figure 4 shows the time taken by the beam to penetrate through different material with varying beam power. The results indicate that the beam will take less time to penetrate any material when the laser beam power increases [28].

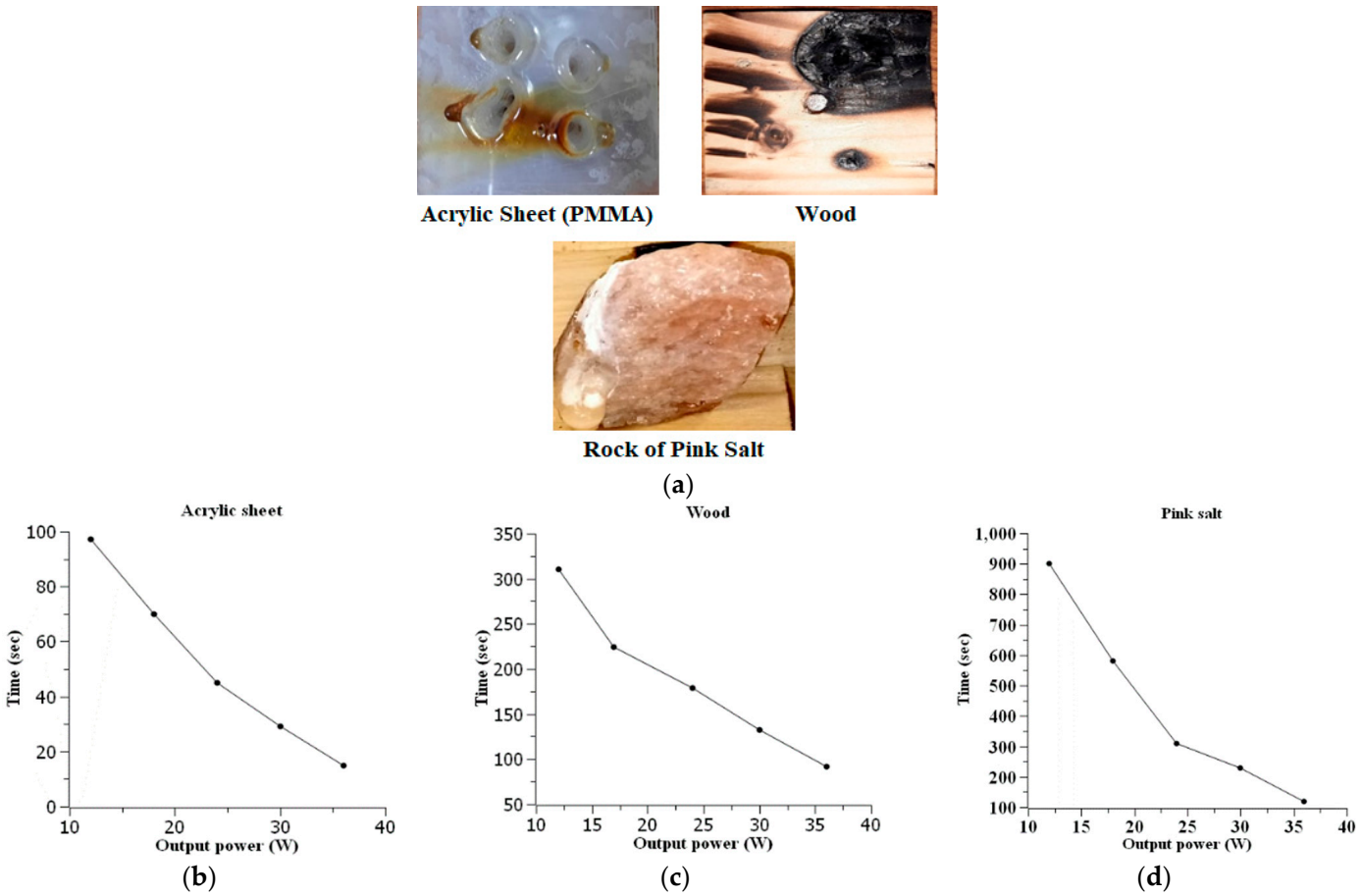

Figure 4. (**a**) Snap of samples after analysis. Penetration time variation along output power for (**b**) acrylic sheet (thickness = 30 mm). (**c**) Wood (thickness = 12 mm). (**d**) Rock of pink salt (thickness = 5 mm).

The graph Figure 5 shows that the penetration rate through the salt, acrylic sheet (PMMA), and wood increases with the output power increase. The penetration rate of the beam through salt and wood is less than that of the acrylic sheet. Most of the laser energy is utilized in burning wood, so the wood's penetration rate is less than the acrylic sheet. The salt rock penetration rate is less because it has a very high melting point, and the beam takes more time to penetrate through the salt rock. The laser penetration rate through the material decreases with increasing melting point because the heat is produced when the laser falls on the material; the material meltdown first and then gets vaporized due to high temperature. Therefore, the laser penetration rate through the rock of pink salt is less than the acrylic sheet (PMMA) [29–31].

The advantage of the laser system described above is that it is low-cost compared to the commercial laser and can easily be controlled and maintained without complication because of its simple design and construction. The laser system can be further used for many potential applications such as laser ablation and melting, for which high power is needed.

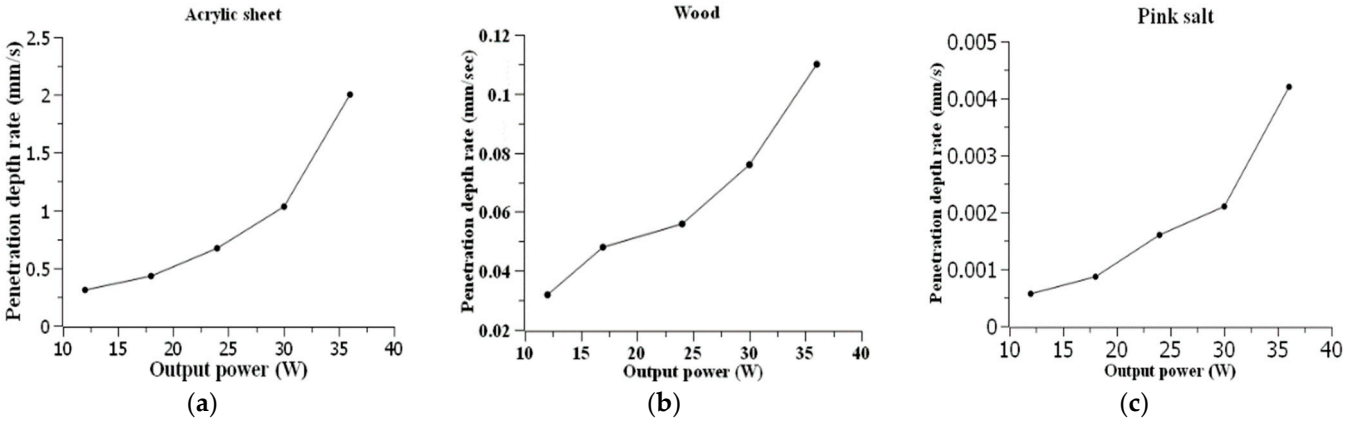

Figure 5. Beam penetration rate along with output power (**a**) acrylic sheet (PMMA) (**b**) wood (**c**) rock of pink salt.

5. Conclusions

Design, construction, and characterization of a very low-cost sealed tube medium power (40 W) CO_2 laser system is presented, consisting of a prototype chiller and flyback-based high voltage power supply. A high-tension pump source is designed to generate the required high voltage in the kilovolts range (8 kV to 30 kV) in the cavity, using the flyback transformer along with its flyback driver circuit. A prototype cooling system is designed and constructed using a thermoelectric cooler (TEC) to maintain the laser cavity temperature. The cooling system can cool down the water up to 8 °C with a cooling rate of 0.7 °C/min, which is enough to compensate for the heat generated by the tube and make it stable for an extended period of its operation. The performance and efficiency of the cooling system at the different laser output power are studied, which shows that the chiller is stable and maintains the cavity temperature during the laser's long-time operation. Comparing power, current, and applied voltage indicates that the current flowing through the tube increases with an increase in the applied voltage so that laser output power increases. The laser beam's penetration rate through the rock of pink salt, wood, and acrylic sheet (PMMA) at different output power is investigated, which shows that increasing the output power increases the penetration rate through the material. The laser penetration rate through the material decreases with increasing melting points because heat is produced when the laser falls on the material. Therefore, the laser penetration rate through the rock of pink salt is less than the acrylic sheet (PMMA) because of its high melting point.

Author Contributions: Conceptualization, T.I., M.N. and A.S.B.; methodology, M.N. and T.I.; software, M.N. and T.I.; validation, T.I., M.N. and A.S.B.; formal analysis, M.N. and T.I.; investigation, M.N.; resources, T.I., M.N. and A.S.B.; data curation, M.N., T.I. and M.H.; writing—original draft preparation, M.N.; writing—review and editing, T.I., M.N. and M.H.; visualization, T.I., M.N.; supervision, T.I. and A.S.B.; project administration, T.I., M.N. and A.S.B.; funding acquisition, T.I. and A.S.B. All authors have read and agreed to the published version of the manuscript.

Funding: This research received no external funding.

Data Availability Statement: The data supporting this study's findings are available within the article.

Conflicts of Interest: On behalf of all authors, the corresponding author states that there is no conflict of interest.

References

1. Verdeyen, J.T. *Laser Electronics*; Prentice-Hall Englewood Cliffs: Hoboken, NJ, USA, 1995.
2. Wang, C.K. Analysis and Applications of Carbon Dioxide Laser. *J. Phys. Conf. Ser.* **2020**, *1634*, 012138. [CrossRef]
3. Fujimoto, J.; Ohta, T.; Nowak, K.M.; Suganuma, T.; Kameda, H.; Moriya, M.; Yokoduka, T.; Fujitaka, K.; Sumitani, A.; Mizoguchi, H. Development of the reliable 20 kW class pulsed carbon dioxide laser system for LPP EUV light source. In *Extreme Ultraviolet (EUV) Lithography II*; SPIE: San Jose, CA, USA, 2011; Volume 7969, pp. 880–890.

4. Patel, C.K.N. Continuous-wave laser action on vibrational-rotational transitions of CO_2. *Phys. Rev.* **1964**, *136*, A1187. [CrossRef]
5. Patel, C.K.N. Selective Excitation Through Vibrational Energy Transfer and Optical Maser Action in N_2-CO_2. *Phys. Rev. Lett.* **1964**, *13*, 617. [CrossRef]
6. Hanst, P.L.; Morreal, J.A. A Wavelength-Selective, Repetitively Pulsed CO_2 Laser. *Appl. Opt.* **1969**, *8*, 109–115. [CrossRef] [PubMed]
7. Thiebeaux, C.; Delahaigue, A.; Courtois, D.; Jouve, P. Design of a low-pressure CW carbon dioxide laser. *Infrared Phys.* **1981**, *21*, 41–44. [CrossRef]
8. Bilida, W.D.; Strohschein, J.D.; Seguin, H.J. High-power 24-channel radial array slab rf-excited carbon dioxide laser. In *Gas and Chemical Lasers and Applications II*; International Society for Optics and Photonics: San Jose, CA, USA, 1997; Volume 2987, pp. 13–21.
9. Nath, A.K.; Reghu, T.; Paul, C.P.; Ittoop, M.O.; Bhargava, P. High-power transverse flow CW CO_2 laser for material processing applications. *Opt. Laser Technol.* **2005**, *37*, 329–335. [CrossRef]
10. Haberberger, D.; Tochitsky, S.; Joshi., C. Fifteen terawatt picosecond CO_2 laser system. *Opt. Express* **2010**, *18*, 17865–17875. [CrossRef] [PubMed]
11. Naeem, M.; Imran, T.; Munawar, R.; Bhatti, A.S. Development of Low-Cost Prototype N2 Laser System and Laser-Induced Fluorescence of Pyranine. *J. Electr. Electron. Eng.* **2022**, *10*, 47–56. [CrossRef]
12. Products Made with Zemax Define Our World. Available online: https://www.zemax.com/ (accessed on 20 December 2021).
13. Naeem, M.; Fatima, N.-U.-A.; Hussain, M.; Imran, T.; Bhatti, A.S. Design Simulation of Czerny–Turner Configuration-Based Raman Spectrometer Using Physical Optics Propagation Algorithm. *Optics* **2022**, *3*, 1–7. [CrossRef]
14. Naeem, M.; Imran, T. Design and Simulation of Mach-Zehnder Interferometer by Using ZEMAX Optic Studio. *Acta Sci. Appl. Phys.* **2022**, *2*, 2–6.
15. Naeem, M.; Imran, T.; Hussain, M.; Bhatti, A.S. Design Simulation and Data Analysis of an Optical Spectrometer. *Optics* **2022**, *3*, 304–312. [CrossRef]
16. Available online: https://www.ni.com (accessed on 1 August 2021).
17. Available online: https://www.multisim.com (accessed on 1 August 2021).
18. Floyd, T.L. *Electronic Devices: Conventional Current Version*; Pearson: London, UK, 2012.
19. Bondarev, A.V.; Fedorov, S.V.; Muravyova, E.A. Control systems with pulse width modulation in matrix converters. *IOP Conf. Ser. Mater. Sci. Eng.* **2018**, *327*, 052008. [CrossRef]
20. Hussain, M.; Imran, T. Design and construction of prototype transversely excited atmospheric (TEA) nitrogen laser energized by a high voltage electrical discharge. *J. King Saud Univ.-Sci.* **2015**, *27*, 233–238. [CrossRef]
21. Hussain, M.; Imran, T. Experimental investigations of an efficient electric pump source for Blumlein-based TEA nitrogen laser. *Int. J. Sci. Eng. Res.* **2017**, *8*, 1214–1219.
22. Hussain, M. Design and Fabrication of Prototype Transversely Excited Atmospheric (TEA) Nitrogen Laser. Ph.D. Thesis, COMSATS Institute of Information Technology Lahore-Pakistan, Lahore, India, 2012.
23. Liu, Y.; Jiang, T.; Yang, Z.; Tai, Y.; Zhang, C. Design and Manufacture of a Pulse Driving Circuit for Semiconductor Laser. In *Advancements in Mechatronics and Intelligent Robotics*; Springer: Singapore, 2021; pp. 441–447.
24. Botero, G.; Gomez, D.; Nisperuza, D.; Bastidas, A. Design and performance of a sealed CO_2 laser for industrial applications. *J. Phys.-Conf. Ser.* **2011**, *274*, 012058. [CrossRef]
25. Khan, N.; Abas, N.; Kalair, A.R.; Mariun, N. A Model of a Repetitively Pulsed Sealed-off CO_2 Laser. *Lasers Eng.* **2018**, *40*, 277–296.
26. Aram, M.; Soltanmoradi, F.; Behjat, A. Investigation on parallel spark array pre-ionization TEA CO2 laser. In *Atomic and Molecular Pulsed Lasers V*; International Society for Optics and Photonics: Bellingham, WA, USA, 2004; Volume 5483, pp. 43–50.
27. Radovanovic, M.; Milos Madic, M. Experimental investigations of CO2 laser cut quality: A review. *Nonconv. Technol. Rev.* **2011**, *4*, 35.
28. Auwal, S.T.; Ramesh, S.; Yusof, F.; Manladan, S.M. A review on laser beam welding of copper alloys. *Int. J. Adv. Manuf. Technol.* **2018**, *96*, 475–490. [CrossRef]
29. Madić, M.; Radovanović, M.; Nedić, B.; Gostimirović, M. CO_2 laser cutting cost estimation: Mathematical model and application. *Int. J. Laser Sci. Fundam. Theory Anal. Methods* **2018**, *1*, 169–183.
30. Mushtaq, R.T.; Wang, Y.; Rehman, M.; Khan, A.M.; Mia, M. State-Of-The-Art and Trends in CO2 Laser Cutting of Polymeric Materials—A Review. *Materials* **2020**, *13*, 3839. [CrossRef]
31. Badoniya, P. CO_2 laser cutting of different materials—A review. *Int. Res. J. Eng. Technol. (IRJET)* **2018**, *5*, 2103–2115.